2022 IEEE 25th International Conference on Intelligent Transportation Systems (ITSC)
October 8-12, 2022, Macau, China

Integrating PDE Observer with Deep Learning for Traffic State Estimation

Chenguang Zhao, Huan Yu

***Abstract*— Traffic state estimation (TSE) refers to the inference of traffic state information from partially observed traffic data and some prior knowledge of the traffic dynamics. TSE plays a key role in traffic management as traffic control relies on an accurate estimation of the traffic states. Macroscopic traffic models describe traffic dynamics with aggregated values such as traffic density, velocity, and flow and are often employed for TSE of a freeway road segment. This paper integrates Partial Differential Equation (PDE) observer design and deep learning paradigm to estimate spatial-temporal traffic states from boundary sensing. With the PDE observer providing an rigorous guarantee for state estimates, we propose Observer-Informed Deep Learning (OIDL) paradigm which is a data-driven solution to TSE that leverages the PDE observer design. An Observer-Informed Neural Network (OINN) is constructed by training NN to generate state estimates and use the boundary observer for regularization. The OINN forms a novel class of data-efficient function approximators that encode PDE observer as theoretical guarantee and improves the accuracy and convergence speed. Experiments using NGSIM data-set demonstrate that the proposed OIDL reduces the estimation error compared to either the model-based observer or either the data-driven neural network. We also compare OIDL with the existing Physics-informed Deep Learning (PIDL) approach for TSE.**

***Index Terms*— Boundary Observer, Traffic State Estimation, Physics-Informed Deep Learning**

I. INTRODUCTION

Freeway traffic management such as ramp metering control, varying speed limits control usually relies on accurate real-time information of traffic states [19]. Freeway traffic conditions can be detected at locations equipped with sensors such as loop detectors and cameras. Due to financial and technical limitations, it is difficult to measure spatially distributed traffic states on the freeway at all times. Therefore, it is important to estimate the full traffic states of a road segment from partial observations, usually referred to as the traffic state estimation (TSE) problem [14]. In particular, boundary observer design is of practical relevance since it estimates the in-domain traffic states from observations at the boundary of a road segment, where traffic states are described with aggregated values such as density, velocity, and flow. Fig. 1 gives an example of TSE by a boundary observer.

Most approaches of boundary observer TSE can be grouped into two categories, model-based [1], [2], [11], [12], [21], [22], [24], [25] and data-driven [8], [15], [23], depending on a priori knowledge of traffic dynamics and the input traffic data they employ. The model-based approaches employ macroscopic traffic models as explicit a priori knowledge to describe the evolution of aggregated traffic states, including the first-order Lighthill-Whitham-Richards (LWR) model [2], and the second-order Aw-Rascle-Zhang (ARZ)model [24]. The widely applied model-based TSE approaches are derived from data assimilation such as Kalman Filter and its variants [11], [12], [21]. The other major approaches mainly focus on solving PDE-based boundary value problems using numerical schemes [1], [22], or control design [24], [25]. When the model is representative, the model-based approach achieves accurate estimation with high interpretability. However, to get such a representative model requires careful calibration from a large volume of traffic data.

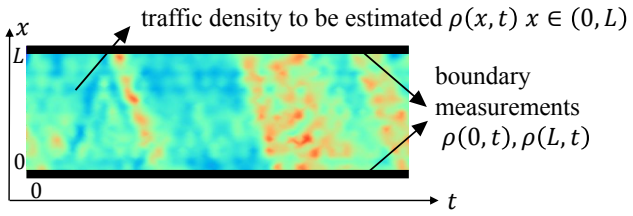

Fig. 1. The boundary observer aims to estimate the macroscopic traffic state in a spatial-temporal region given boundary observations. In this figure we use traffic density as an example.

The data-driven approaches make no explicit assumptions on the traffic dynamics and rely on historical traffic data. It works as a black box to capture the traffic dynamics directly from historical and current observation. The data-driven TSE has been extensively studied such as linear regression [15], Bayesian network[8], deep learning [23]. Compared with model-based approaches, the data-driven methodologies automatically learn the traffic dynamics from data and thus could overcome the limitations of a manually calibrated model. However, one main drawback of the data-driven TSE approaches lies in their lack of interpretability and generalization. For example, some neural-network-based algorithms might give unreasonable estimations when NN is trained on some training data and the real traffic presents a different pattern with the training data [10].

To combine the strength of model-based and data-driven approaches, hybrid frameworks have received considerable attention. Raissi et al. [13] propose a general structure, Physics Informed Deep Learning (PIDL), to solve Boundary Value Problem or Initial Value Problem of PDEs using neural networks. The integration of physical models and machine learning has received increased attention in a number of applications, such as underground reservoir pressure man-

* Huan Yu is corresponding author. Email:*huanyu@ust.hk*
Huan Yu and Chenguang Zhao are with the Hong Kong University of Science and Technology (Guangzhou), Thrust of Intelligent Transportation, Nansha, Guangzhou, 511400, Guangdong, China. Huan Yu is also affiliated with the Hong Kong University of Science and Technology, Department of Civil and Environmental Engineering, Hong Kong SAR, China.

2022 IEEE 25th International Conference on Intelligent Transportation Systems (ITSC) | 978-1-6654-6880-0/22/$31.00 ©2022 IEEE | DOI: 10.1109/ITSC55140.2022.9922409

agement, [6], climate change forecasting [9], and battery modeling [20]. Huang et al. [7], and Shi et al. [16], [17], [18] applied PIDL hybrid approaches to achieve TSE with distributed loop detectors among the road.

In this paper, we propose a novel hybrid TSE framework combining a designed PDE boundary observer [24] and deep learning paradigm [13], which has not been studied before to the best of authors' knowledge. We develop a PDE Observer informed Deep Learning (OIDL) approach to estimate in-domain traffic states with only boundary sensing. The previous hybrid frameworks [7], [18] use multiple distributed loop detectors for TSE on a road segment whereas the proposed OIDL only requires sensors at two boundaries. The decrease in the measurements poses new challenges to the estimation since less information on the traffic dynamics is revealed. Beyond solving boundary value problems for macroscopic traffic PDE, the OIDL approach approximates the PDE boundary observer which is designed to analytically predict the real-time traffic simply from boundary measurements. The main contributions are summarized as:

- The proposed OIDL approach estimates in-domain traffic states with only boundary sensing. An observer uninformed neural network uses boundary observations as TSE input and its output is regularized by the PDE observer provided as rigorous estimation guarantees. The PDE observer estimation errors converge to zeros in finite time.
- We perform experiments on the NGSIM data-set, and the result shows that the proposed OIDL reduces the estimation error for density and speed by 5% and 15% compared with the pure model-based boundary observer.
- We also compare OIDL with the state-of-the-art hybrid framework PIDL. Experiments show that the OIDL not only increases the estimation accuracy but also reduces the computation burden.

II. Model-based Boundary Observer

We consider the evolution of the traffic dynamics on a road segment of the length of L. The spatial-temporal domain is $\mathcal{D} = \{(x,t)|0 \le x \le L, t \ge 0\} \subset \mathbb{R}^2$. A macroscopic model can be written in the general form of

$$\partial_t \boldsymbol{u}(x,t) + \mathcal{N}[\boldsymbol{u}(x,t);\boldsymbol{\omega}] = 0, \quad (x,t) \in \mathcal{D}, \tag{1}$$

where $\boldsymbol{u}(x,t)$ is aggregated traffic states like traffic flow q, density ρ, speed v; $\mathcal{N}$ is a general non-linear differential operator parametrized by $\boldsymbol{\omega}$. In this section, we will first give the second-order ARZ model, and then introduce the designed observer [24].

A. ARZ model

The ARZ model is a second-order macroscopic model, governing the evolution of traffic density $\rho(x,t)$ and traffic velocity $v(x,t)$

$$\partial_t \rho + \partial_x(\rho v) = 0, \tag{2}$$

$$\partial_t(\rho(v - V(\rho))) + \partial_x(\rho v(v - V(\rho))) = -\frac{\rho(v - V(\rho))}{\tau}, \tag{3}$$

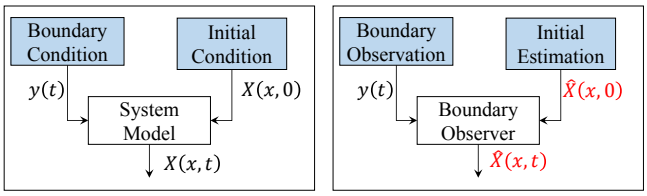

Fig. 2. A comparison of the ARZ model and the boundary observer. Given initial conditions $\rho(x,0), v(x,0)$ and boundary conditions $\rho(0,t), v(0,t), \rho(L,t), v(L,t)$, a well-defined solution of the ARZ model $\rho(x,t), v(x,t)$ can be derived. The boundary observer, on the other side, aims to estimate the in-domain solution given only boundary observations. The boundary observer should be designed such that given an inaccurate initial estimation $\hat{\rho}(x,0), \hat{v}(x,0)$, the estimated states $\hat{\rho}(x,t), \hat{v}(x,t)$ converges to the $\rho(x,t), v(x,t)$.

where $V(\rho)$ and τ are the two parameters. $V(\rho)$ denotes equilibrium velocity-density relationship, and τ is relaxation time which describes the drivers' behavior adapting to the equilibrium relation $V(\rho)$ over time. The equilibrium relationship $V(\rho)$ is chosen to satisfy two conditions: a) $V(\rho)$ is a decreasing function of density ρ, i.e., $V'(\rho) > 0$; and b) the equilibrium flow function $Q(\rho) = \rho V(\rho)$ is concave, i.e., $Q''(\rho) \le 0$. One basic choice of $V(\rho)$ is the Greenshield's model, $V(\rho) = v_f - v_f(\rho/\rho_m)$, where ρ_m is the maximum density and v_f is the maximum velocity.

B. Boundary observer design beyond PDE model

Backstepping design is a classical method for control and estimation of PDE systems and was employed to design the Luenburger-type boundary observer in [24]. In Fig. 2, we give a comparison of the model-based forward solution and the boundary observer. To have a unique well-defined solution of the ARZ model, both initial conditions and boundary conditions should be specified. The boundary observer, on the other side, aims to estimate the in-domain traffic states with only boundary observations. In [24], we design a boundary observer such that the estimated states $\hat{\rho}(x,t), \hat{v}(x,t)$ converge to the ground truth given any bounded initial estimation $\hat{\rho}(x,0), \hat{v}(x,0)$. We only provide the PDE observer formulation in this paper. Detailed mathematical derivations can be found in [24].

We take the measurement of boundary values of the traffic density and velocity at $x = 0$ and $x = L$ as in (4), (5),

$$y^{\rho}_{\text{in}}(t) = \rho(0,t), \qquad y^{v}_{\text{in}}(t) = v(0,t), \tag{4}$$

$$y^{\rho}_{\text{out}}(t) = \rho(L,t), \qquad y^{v}_{\text{out}}(t) = v(L,t). \tag{5}$$

The PDE observer is given by

$$\partial_t \hat{\rho} + \partial_x(\hat{\rho}\hat{v}) = E_\omega, \tag{6}$$

$$\partial_t \hat{v} + (\hat{v} + \hat{\rho}V'(\hat{\rho}))\,\partial_x \hat{v} = \frac{V(\hat{\rho}) - \hat{v}}{\tau} + E_v, \tag{7}$$

$$\hat{\rho}(0,t) = \frac{y^{\rho}_{\text{in}}(t) y^{v}_{\text{in}}(t)}{\hat{v}(0,t)}, \tag{8}$$

$$\hat{v}(L,t) = y^{v}_{\text{out}}(t), \tag{9}$$

where $\hat{\rho}(x,t)$ and $\hat{v}(x,t)$ are the estimated traffic density and speed respectively, E_ω and E_v are the designed output injection terms that are used to correct the estimation based on the boundary measurements. The general form of E_ω

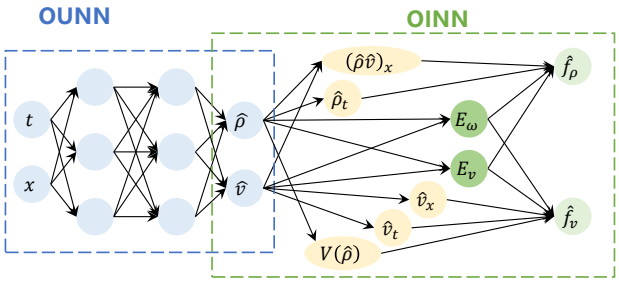

Fig. 3. In the proposed OIDL paradigm, OUNN generates traffic state estimates $\hat{\rho}, \hat{v}$ by taking boundary data as the input, then OINN regulates the purely data-driven estimation by a residual value $\hat{f}$ that is designed based on the boundary observer.

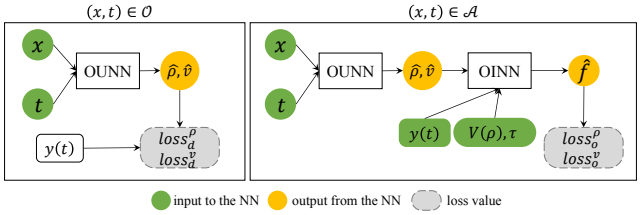

Fig. 4. Data-flow in the OIDL. For the observation sets $\mathcal{O}$, only the OUNN is used to calculate the loss value. While for the auxiliary sets $\mathcal{A}$, both OUNN and OINN are involved. For both $\mathcal{O}$ and $\mathcal{A}$, only indexes (x,t) are required. The observed boundary traffic states $y(t) = [y_{\text{in}}^\rho(t), y_{\text{out}}^\rho(t), y_{\text{in}}^v(t), y_{\text{out}}^v(t)]$ are given in $\mathcal{P}$.

and E_v can be written as a function of the estimation $\hat{\rho}(x,t), \hat{v}(x,t)$, the observation $y_{\text{in}}^\rho(t), y_{\text{out}}^\rho(t), y_{\text{in}}^v(t), y_{\text{out}}^v(t)$, and the model parameters V, τ,

$$E_\omega = E_\omega\left(\hat{\rho}(x,t), \hat{v}(x,t), y_{\text{in}}^\rho(t), y_{\text{out}}^\rho(t), y_{\text{in}}^v(t), y_{\text{out}}^v(t), V, \tau\right), \tag{10}$$

$$E_v = E_v\left(\hat{\rho}(x,t), \hat{v}(x,t), y_{\text{in}}^\rho(t), y_{\text{out}}^\rho(t), y_{\text{in}}^v(t), y_{\text{out}}^v(t), V, \tau\right). \tag{11}$$

The detailed formulation of the output injection terms E_ω and E_v is referred to [24]. With the designed E_ω and E_v, we have the following theorem [24] stating its stability.

Theorem 1: Consider the estimated system with initial condition $\rho(x,0) - \hat{\rho}(x,0) \in L^2([0,L]), v(x,0) - \hat{v}(x,0) \in L^2([0,L])$, the estimation error is exponentially stable in the L^2 sense. It holds that

$$\|\rho(\cdot,t) - \hat{\rho}(\cdot,t)\| \to 0, \tag{12}$$

$$\|v(\cdot,t) - \hat{v}(\cdot,t)\| \to 0, \tag{13}$$

and the estimation errors converge to zero within finite time [24].

III. Observer-informed Deep Learning Paradigm

The proposed OIDL consists of two parts, an Observer Uninformed Neural Network (OUNN) to estimates the traffic state by a neural network; and an Observer Informed Neural Network (OINN) to regularize the estimation output of OUNN. The OIDL is optimized to meet two objectives. From the data-driven perspective, traffic state estimates should be as close as possible to some observation data. From the model-driven perspective, the estimation is aimed at approximating the PDE observer on some training data which are theoretical constraints for traffic state estimates of OUNN. Two types of training data are introduced to realize these two objectives respectively, observation points and auxiliary points.

1) Observation Points $\mathcal{O} = \{0, L\} \times [0, T]$ representing the (location, time) where and when each observation is obtained, and observed boundary traffic states $\mathcal{P} = \{y_{\text{in}}^\rho(t), y_{\text{out}}^\rho(t), y_{\text{in}}^v(t), y_{\text{out}}^v(t)\}$ recording the observed traffic density and speed at the boundary of the considered road segment. The OUNN takes location x, time t indexes as inputs and outputs estimated traffic density $\hat{\rho}(x,t;\theta)$ and speed $\hat{v}(x,t;\theta)$ with θ being the trainable weight parameters of the OUNN. We aim to minimize the errors between estimated traffic states and the measured data at boundaries, so the data loss is defined as

$$loss_d^\rho = \frac{1}{O} \sum_{(x,t)\in\mathcal{O}} (\rho(x,t) - \hat{\rho}(x,t;\theta))^2, \tag{14}$$

$$loss_d^v = \frac{1}{O} \sum_{(x,t)\in\mathcal{O}} (v(x,t) - \hat{v}(x,t;\theta))^2, \tag{15}$$

where $O = |\mathcal{O}|$ denotes the number of observation points.

2) Auxiliary points $\mathcal{A} = \{(x,t)\} \subset \mathcal{D}_f$, where $\mathcal{D}_f = [0,L] \times [0,T]$ is a spatial-temporal domain. The estimated states predicted by OIDL are regularized by the designed boundary observer, that is, approximating the observer's prediction. And auxiliary points $\mathcal{A}$ are the ones randomly selected from the whole spatial-temporal domain, on which the observer loss is defined as

$$loss_o^\rho = \frac{1}{A} \sum_{(x,t)\in\mathcal{A}} |\hat{f}_\rho(x,t,\hat{\rho}(x,t;\theta))|^2, \tag{16}$$

$$loss_o^v = \frac{1}{A} \sum_{(x,t)\in\mathcal{A}} |\hat{f}_v(x,t,\hat{v}(x,t;\theta))|^2, \tag{17}$$

where $\hat{f}_\rho$ and $\hat{f}_v$ denote the residual value for state estimates $\hat{\rho}$ and $\hat{v}$,

$$\hat{f}_\rho = \partial_t\hat{\rho} + \partial_x(\hat{\rho}\hat{v}) - E_\omega, \tag{18}$$

$$\hat{f}_v = \partial_t\hat{v} + (\hat{v} + \hat{\rho}V'(\hat{\rho}))\,\partial_x\hat{v} - \frac{V(\hat{\rho}) - \hat{v}}{\tau} - E_v. \tag{19}$$

If the state estimates perfectly agree with the PDE observer, the residual values become zeros.

In Fig.4, we present a diagram for the calculation process of these two types of loss. To consider both the data loss and the observer loss, the overall loss function is then defined as

$$loss = \alpha_\rho loss_d^\rho + \alpha_v loss_d^v + \beta_\rho loss_o^\rho + \beta_v loss_o^v, \tag{20}$$

with $\alpha_\rho, \alpha_v, \beta_\rho, \beta_v$ being non-negative coefficients to balance the trade-off between data discrepancy and observer discrepancy. With a higher α, the OIDL puts more trust in the observed data by training NN to reduce the data discrepancy

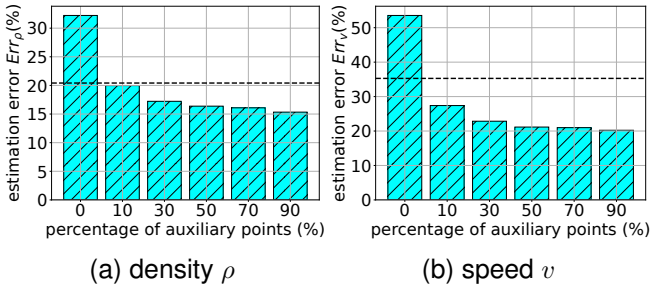

Fig. 5. Estimation error under different percentages of auxiliary points. The dotted line is the estimation error obtained by the pure model-based boundary observer.

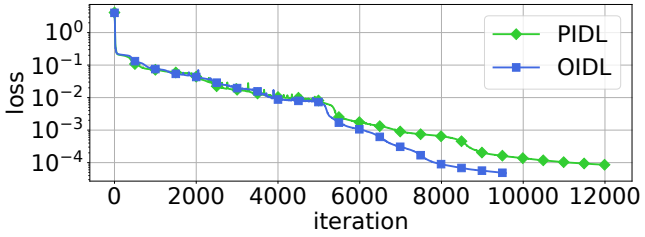

Fig. 6. The loss curve for OIDL and PIDL. It can be seen that the proposed OIDL reduces the loss value by approximately $10^{-0.5}$, and also takes nearly 15% fewer iterations to converge.

as much as possible, whereas with a higher β, the OIDL puts more trust in the theoretically derived observer.

The hybrid approach for TSE is also studied in related work [7], [18] where PIDL is adopted.The key idea of PIDL is to compute a data-driven solution to the initial value boundary problem (IVBP) of PDEs as in Fig. 2. Only when both the initial condition $\rho(x,0), v(x,0)$, and the boundary condition among $\rho(0,t),\ v(0,t), \rho(L,t),\ v(L,t)$ are given, there exist a unique and well-posed solution of the density and velocity solution $\rho(x,t), v(x,t)$ governed by the ARZ PDE model (2)-(3). If PIDL is applied for TSE and initial condition data is not used for observations, there does not exist a unique and well-posed solution from model regularization. As a result, the state estimates of PIDL could vary along with the intial conditions. In contrast, our OIDL does not specify the initial condition as long as the initial estimation errors are within some range as stated in Theorem 1. The PDE boundary observer is able to recover state estimates simply from boundary measurements. This property could greatly compensate the drawbacks of NN with regards to its sensitivity to the change of initial conditions and the difficulty of optimizing hyper-parameters when training NN.

IV. Experiment

To test the performance of the proposed OIDL, we implement simulation experiments on the NGSIM data-set [4]. We first give the experiment settings and then analyze the results to investigate the performance of the proposed OIDL.

A. Experiment setup

The NGSIM data-set collects the vehicles' trajectory on a highway in Emeryville, CA, USA. We adopt Edie's formula

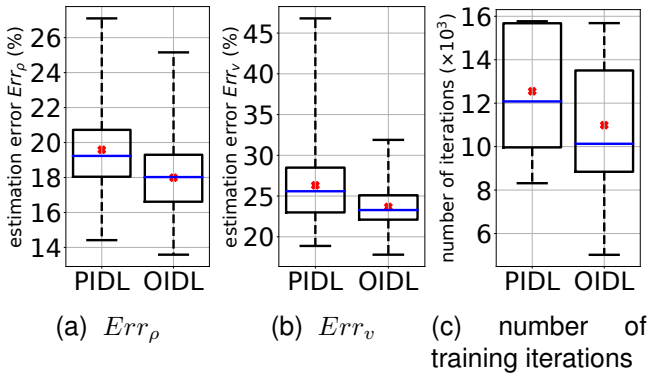

Fig. 7. The boxplot of the estimation error and the number of iterations for OIDL and PIDL. The red 'X' is the average. The blue line is the median, and the two short lines are the minimum and maximum iterations. The low and top boundaries of the box are the first and third quartile respectively.

[3] to transform the microscopic vehicle trajectory data into macroscopic traffic states. For the continuous spatial-temporal domain $\mathcal{D}_f = [0,L] \times [0,T]$, we divide it into $N_x \times N_t$ cells, with each cell having space interval $\Delta x = L/N_x$ and time interval $\Delta t = T/N_t$. Denote the discrete spatial-temporal domain as $\mathcal{G} = \{(i_x \cdot \Delta x, i_t \cdot \Delta t) | i_x \in [N_x], i_t \in [N_t]\}$. We take a region of $L = 480\,\text{m}$, $T = 750\,\text{s}$, and discrete it with $\Delta x = 20\,\text{m}$, $\Delta t = 15\,\text{s}$, $N_x = 24$, and $N_t = 50$.

We adopt a fully connected neural network with 8 hidden layers and 50 neons in each hidden layer as the OUNN. We utilize the Xavier uniform initializer [5] to initialize the weight parameters of the OUNN. For a hidden layer with input-dimension n_{in} and output-dimension n_{out}, its weight variables are initialized based on the uniform distribution between $-\sqrt{\frac{6}{n_{in}+n_{out}}}$ and $\sqrt{\frac{6}{n_{in}+n_{out}}}$. To train the OUNN parameters θ, we firstly run ADAM for 5,000 epochs for rough training. Then we adopt L-BFGS to refine the NN. The training will terminate when the change in loss during two consecutive steps is smaller than 10^{-6}.

We adopt the data collected between 04:00 and 04:15 to calibrate the equilibrium velocity-density relationship $V(\rho)$. The relaxation time τ is taken as $30\,\text{s}$, as suggested in the previous work [24].

B. Estimation results of OIDL

To analyze the estimation of the proposed OIDL, we take the L^2 error to evaluate the estimation accuracy,

$$Err_\rho = \sqrt{\frac{1}{LT}\int_0^T \int_0^L \left(\frac{\rho(x,t) - \hat{\rho}(x,t)}{\rho^*}\right)^2 dxdt}, \quad (21)$$

$$Err_v = \sqrt{\frac{1}{LT}\int_0^T \int_0^L \left(\frac{v(x,t) - \hat{v}(x,t)}{v^*}\right)^2 dxdt}, \quad (22)$$

where ρ^* and v^* are the average of the ground truth.

We have run experiments under different percentages of auxiliary points $\mathcal{A}$. In Fig. 5, we give the estimation error for density and speed with a varying number of auxiliary points. From the figure, the following findings can be made:

- First, the proposed OIDL reduces the estimation error, compared to both pure model-based boundary observer

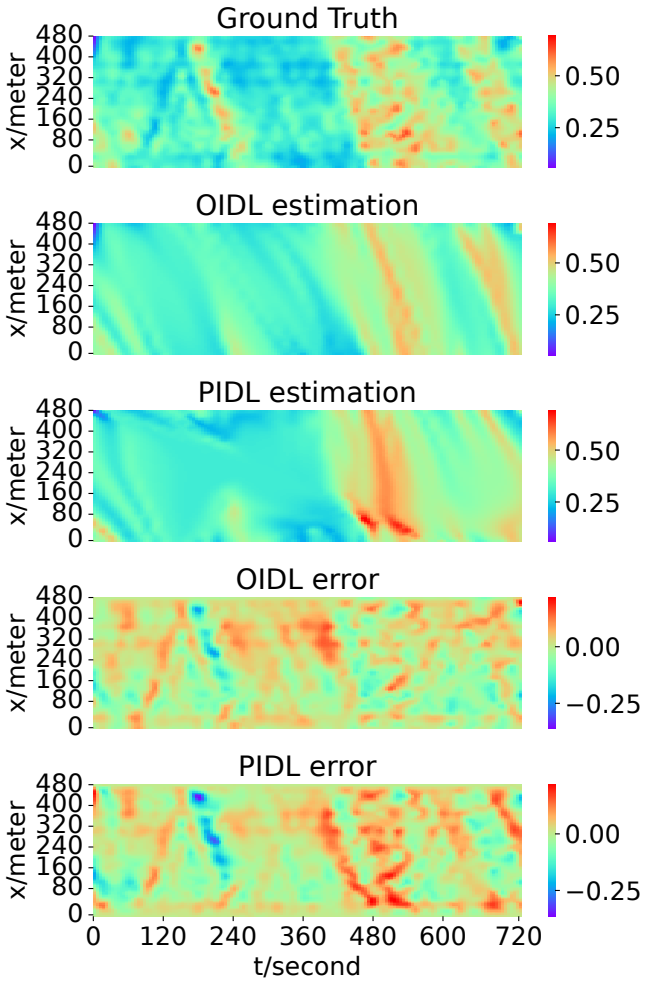

Fig. 8. Ground truth ρ, estimation $\hat{\rho}$, and estimation error $\hat{\rho}-\rho$ of traffic density. (The unit of the color-bar is number of vehicles per meter.)

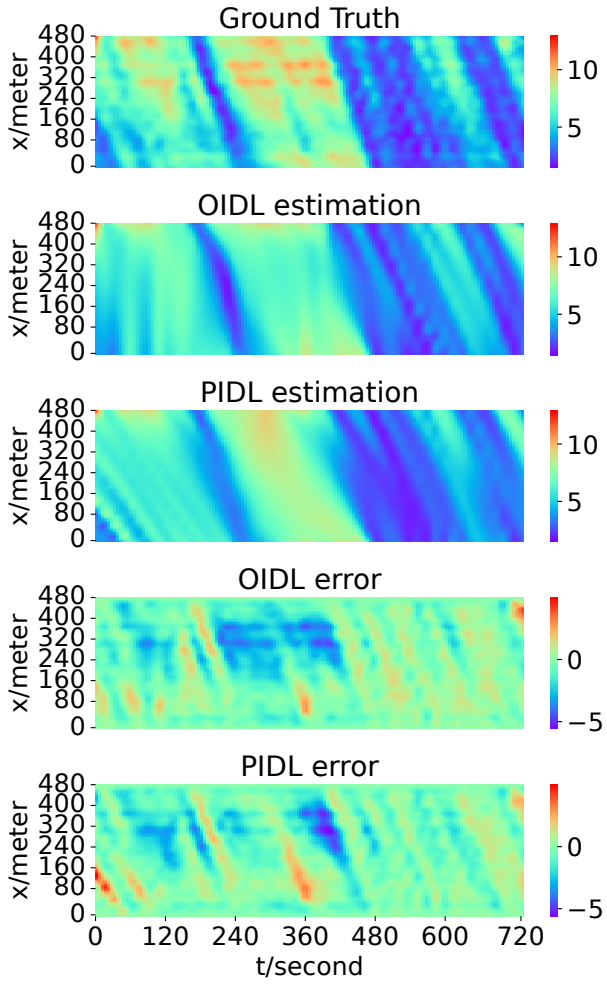

Fig. 9. Ground truth v, estimation $\hat{v}$, and estimation error $\hat{v}-v$ of speed. (The unit of the color-bar is $\mathrm{m/s}$.)

and pure data-driven neural network OUNN. In Fig. 5, the dashed horizontal line represents the estimation error obtained by the boundary observer. And the leftmost bar with no auxiliary points is the estimation error for OUNN. Under all percentages of auxiliary points, the proposed OIDL obtains lower estimation error for both density ρ and speed v, which demonstrates its effectiveness.

- Second, with the increasing of auxiliary points, the estimation error will decrease. Recall that the auxiliary points are included to regularize the estimation output from the OUNN. And with more auxiliary points, the estimation in more (location, time) are utilized to regularize the output by the neural network, and therefore the estimated states will agree with the boundary observer more.

We then compare the proposed OIDL with the state-of-the-art PIDL [18], which takes the ARZ model to regularize the estimation of a neural network. The experiments of OIDL and PIDL are taken under the same settings, including initial weights θ of the NN, auxiliary points $\mathcal{A}$, and model parameters $V(\rho)$ and τ. In Fig. 6, the loss value during the training process is given. It can be seen that the proposed OIDL takes only 10k iterations to converge to the loss value of $10^{-4.5}$, The PIDL takes 12k iterations to converge, and the final loss value is 10^{-4}.

We then run 100 experiments with random initial weights of the neural network and different coefficient β/α. In Fig. 7, we give the boxplot of the estimation error and the number of iterations of OIDL and PIDL. From Fig. 7, the proposed OIDL not only increases the estimation error, but also reduces the computation burden.

- The OIDL reduces the estimation error for both density ρ and speed v. From Fig. 7, the estimation errors obtained by OIDL are $Err_\rho = 17.99\%$, $Err_v = 23.67\%$ for density and speed respectively, while for PIDL the errors are $Err_\rho = 19.59\%$ and $Err_v = 26.31\%$.
- The maximum possible iterations for OIDL and PIDL are approximately the same, around 16k. But the average number of the iterations taken by the proposed OIDL is 10k, which is lower than the 12k of the PIDL. Therefore, the proposed PIDL converges faster, alleviating the burden of computation.

To further investigate the estimation in more detail, we

select the estimated traffic state with the lowest L^2 error for OIDL and PIDL, and draw the heat-map of the ground truth, estimated result, and estimation error in Fig. 8 and 9 for traffic density and speed respectively. Compared to the ground truth, the PIDL may give misleading estimations. For example, for the estimated and ground-truth traffic density ρ in Fig. 8, near the area $(x = 90\,\mathrm{m}, t = 310\,\mathrm{s})$, false congestion or even collision is expected to happen by PIDL.

From Fig. 7, 8, and 9, we can see that the proposed OIDL obtains a more accurate estimation. The main reason is stated as follows. In our experiments, since we have kept all other experiment settings the same for PIDL and OIDL, the main difference between these two hybrid frameworks lies in the PDE model-based solution used to regularize the estimation by the neural network. The PIDL adopts the initial-boundary value solution of the ARZ model as regularization, whereas the proposed OIDL uses the designed boundary observer. If the IVBP solution of the ARZ model is used as regularization, the change of initial condition affects the estimation result. Even prescribed with the same boundary conditions, the in-domain traffic states solution will be different when the initial condition changes. In contrast, the proposed boundary observer can converge to the PDE solution within finite time as long as the initial estimation error is within some range [24]. The initial estimation is calculated as the output of OUNN. With different initial weights of the neural network, the proposed OIDL can reduce the estimation error by the designed output injection terms, and therefore shorten the training process and increase the estimation accuracy.

V. CONCLUSIONS

In this paper, we take the first step towards combining the model-based boundary observer with the deep learning paradigm. A boundary observer with a convergence guarantee is adopted to regulate the training process of a neural network, and a novel OIDL is proposed. Experiments on the NGSIM data-set demonstrate that the OIDL reduces the estimation error for both traffic density and speed compared to the pure model-based boundary observer or the pure data-driven deep learning. Compared with state-of-the-art hybrid approaches for TSE, The proposed OIDL also increases the estimation accuracy and reduces the computation burden.

This paper could have several promising future directions. First, similar to most deep learning frameworks, the optimization of hyper-parameters will be a challenge for OIDL. Second, the boundary observer is formulated under congested traffic scenarios, and TSE under the free-flow regime, or even mixed free and congested regime, requires further investigation. Third, under noisy measurements, the robustness of the structure remains to be an open problem.

REFERENCES

[1] M. Barreau, A. Selivanov, and K. H. Johansson, "Dynamic traffic reconstruction using probe vehicles," in *2020 59th IEEE Conference on Decision and Control (CDC)*. IEEE, 2020, pp. 233–238.

[2] C. G. Claudel and A. M. Bayen, "Guaranteed bounds for traffic flow parameters estimation using mixed lagrangian-eulerian sensing," in *2008 46th Annual Allerton Conference on Communication, Control, and Computing*. IEEE, 2008, pp. 636–645.

[3] L. C. Edie *et al.*, *Discussion of traffic stream measurements and definitions*. Port of New York Authority New York, 1963.

[4] FHWA, "Next Generation Simulation (NGSIM)," 2007. [Online]. Available: https://ops.fhwa.dot.gov/trafficanalysistools/ngsim.htm

[5] X. Glorot and Y. Bengio, "Understanding the difficulty of training deep feedforward neural networks," in *Proceedings of the thirteenth international conference on artificial intelligence and statistics*. JMLR Workshop and Conference Proceedings, 2010, pp. 249–256.

[6] D. R. Harp, D. O'Malley, B. Yan, and R. Pawar, "On the feasibility of using physics-informed machine learning for underground reservoir pressure management," *Expert Systems with Applications*, vol. 178, p. 115006, 2021.

[7] J. Huang and S. Agarwal, "Physics informed deep learning for traffic state estimation," in *2020 IEEE 23rd International Conference on Intelligent Transportation Systems (ITSC)*. IEEE, 2020, pp. 1–6.

[8] J. Jin and X. Ma, "A non-parametric bayesian framework for traffic-state estimation at signalized intersections," *Information Sciences*, vol. 498, pp. 21–40, 2019.

[9] K. Kashinath, M. Mustafa, A. Albert, J. Wu, C. Jiang, S. Esmaeilzadeh, K. Azizzadenesheli, R. Wang, A. Chattopadhyay, A. Singh *et al.*, "Physics-informed machine learning: case studies for weather and climate modelling," *Philosophical Transactions of the Royal Society A*, vol. 379, no. 2194, p. 20200093, 2021.

[10] Y. Liang, Z. Cui, Y. Tian, H. Chen, and Y. Wang, "A deep generative adversarial architecture for network-wide spatial-temporal traffic-state estimation," *Transportation Research Record*, vol. 2672, no. 45, pp. 87–105, 2018.

[11] L. Mihaylova, R. Boel, and A. Hegyi, "An unscented Kalman filter for freeway traffic estimation," *IFAC Proceedings Volumes*, vol. 39, no. 12, pp. 31–36, 2006.

[12] ——, "Freeway traffic estimation within particle filtering framework," *Automatica*, vol. 43, no. 2, pp. 290–300, 2007.

[13] M. Raissi, P. Perdikaris, and G. E. Karniadakis, "Physics-informed neural networks: A deep learning framework for solving forward and inverse problems involving nonlinear partial differential equations," *Journal of Computational Physics*, vol. 378, pp. 686–707, 2019.

[14] T. Seo, A. M. Bayen, T. Kusakabe, and Y. Asakura, "Traffic state estimation on highway: A comprehensive survey," *Annual reviews in control*, vol. 43, pp. 128–151, 2017.

[15] Z. Shan, D. Zhao, and Y. Xia, "Urban road traffic speed estimation for missing probe vehicle data based on multiple linear regression model," in *16th International IEEE Conference on Intelligent Transportation Systems (ITSC 2013)*. IEEE, 2013, pp. 118–123.

[16] R. Shi, Z. Mo, and X. Di, "Physicsinformed deep learning for traffic state estimation: A hybrid paradigm informed by second-order traffic models," in *Proceedings of the AAAI Conference on Artificial Intelligence*, vol. 35, no. 1, 2021, pp. 540–547.

[17] R. Shi, Z. Mo, K. Huang, X. Di, and Q. Du, "Physics-informed deep learning for traffic state estimation," *arXiv preprint arXiv:2101.06580*, 2021.

[18] ——, "A physics-informed deep learning paradigm for traffic state and fundamental diagram estimation," *IEEE Transactions on Intelligent Transportation Systems*, 2021.

[19] S. Siri, C. Pasquale, S. Sacone, and A. Ferrara, "Freeway traffic control: A survey," *Automatica*, vol. 130, p. 109655, 2021.

[20] H. Tu, S. Moura, Y. Wang, and H. Fang, "Integrating physics-based modeling with machine learning for lithium-ion batteries," *arXiv preprint arXiv:2112.12979*, 2021.

[21] Y. Wang and M. Papageorgiou, "Real-time freeway traffic state estimation based on extended Kalman filter: a general approach," *Transportation Research Part B: Methodological*, vol. 39, no. 2, pp. 141–167, 2005.

[22] Y. Wang, M. Zhao, X. Yu, Y. Hu, P. Zheng, W. Hua, L. Zhang, S. Hu, and J. Guo, "Real-time joint traffic state and model parameter estimation on freeways with fixed sensors and connected vehicles: State-of-the-art overview, methods, and case studies," *Transportation Research Part C: Emerging Technologies*, vol. 134, p. 103444, 2022.

[23] D. Xu, C. Wei, P. Peng, Q. Xuan, and H. Guo, "GE-GAN: A novel deep learning framework for road traffic state estimation," *Transportation Research Part C: Emerging Technologies*, vol. 117, p. 102635, 2020.

[24] H. Yu, Q. Gan, A. Bayen, and M. Krstic, "PDE traffic observer validated on freeway data," *IEEE Transactions on Control Systems Technology*, vol. 29, no. 3, pp. 1048–1060, 2020.

[25] L. Zhang and Y. Lu, "Distributed consensus-based boundary observers for freeway traffic estimation with sensor networks," in *2020 American Control Conference (ACC)*. IEEE, 2020, pp. 4497–4502.